Elemental fractionation and stoichiometric sampling in femtosecond laser ablation

Carmen C. Garcia,*[a] Helmut Lindner,[a] Alex von Bohlen,[a] Cedomil Vadla[b] and Kay Niemax[a]

Received 7th December 2007, Accepted 14th January 2008
First published as an Advance Article on the web 14th February 2008
DOI: 10.1039/b718845e

Elemental fractionation in femtosecond laser ablation is studied by ICP-MS by applying successive single laser shots to binary metallic and semiconductor samples as well as to multi-component glasses. Fractionation can be observed in the first laser shots in particular if the laser fluence is near the ablation threshold of the sample. However, the element ratio in the laser-sampled masses changes from shot to shot until it reaches an asymptotic fluence-independent value representing stoichiometric sampling. The asymptotic stoichiometric ratios can be obtained with fewer shots if higher laser fluences are applied. It is shown by electron probe X-ray analysis that different elemental ablation probabilities modify the element compositions in the surface layers of the laser craters until equilibrium conditions are obtained. These conditions can be reached by applying many shots of low laser fluence or with one high-fluence laser shot only. The experimental data reveal that in most cases the elemental ablation probability can be correlated with the respective ionization energies of the elements, *i.e.*, the elements with lower first ionization energy have higher ablation probability. No or only very weak fractionation was observed when elements with nearly the same ionization energies were sampled.

Introduction

Laser ablation inductively coupled plasma mass spectrometry (LA-ICP-MS) is a popular technique for elemental analysis of solid material. From its first introduction in 1985[1] it has shown its benefits in many successful applications.[2–4] Nevertheless, LA-ICP-MS usually requires matrix-matched standards for calibration that are very often not available and, therefore, prevents the method from being even more popular.

There are three main processes responsible for the need for matrix-matched standards. The first is the laser ablation process itself causing fractional ablation of the elements and modifications of the elemental composition in the bottom layers of the craters. The second is the transport of the aerosol generated in the ablation process, where any loss of particle mass during the transport to the ICP can increase the error of the measurement since the elemental compositions of laser generated aerosol particles are size dependent.[5,6] The third process is connected with the atomization of the particles in the ICP and possible changes of the plasma parameters. The requirements in the atomization step are that (i) the particles have to be small enough to be completely atomized during their transit through the ICP and (ii) the total aerosol mass should not significantly change the ionization temperature in the plasma.

Recently, the transport efficiency of particles generated by femtosecond laser ablation (fs-LA) of solid samples has been found to be near to 100%, and independent of the ablation cell geometry and the noble gas (He, Ar) applied as the cell and transport gas.[7,8] These results were not unexpected, since fs-laser produced particles are in the diameter range 5 nm to 3 μm.[5,6] Particles of such sizes can be transported without diffusion or inertial losses over large distances.[9] Therefore, a transport efficiency of near unity was also found by numerical simulations of the particle transport from a particular ablation cell with very short washout times.[10]

The implication of an almost 100% transport efficiency and complete atomization of such fine particles in the ICP is that non-matrix-matched calibration of fs-LA-ICP spectrometry should be possible. This was recently demonstrated by fs-LA-ICP-OES[11] and fs-LA-ICP-MS[12] in our laboratory. However, it was also shown in ref. 12 and by Koch *et al.*[13] that elemental fractionation, which has been studied in nanosecond laser ablation (ns-LA) for many years (see, *e.g.* ref. 14–17), is also an issue in fs-LA. For example, it was found that the Zn/Cu[12,13] and Pb/U[13] ratios increased with laser fluence while the U/Th ratio[13] was almost independent of the fluence. We like to note that Koch *et al.*[13] also observed changes of the Zn/Cu and Pb/U ratios (while the U/Th ratio was unchanged) when the particle concentration in the ICP was varied. In the present paper we will assume that the "mass load" effect can be neglected since it was not observed in our recent publications[7,12] within the bounds of experimental error.

Elemental fractionation is often observed if sampling is performed near to the ablation threshold. For example, Cromwell and Arrowsmith[14] found that the ICP-MS ion signals of Pb, Zn, Sn and Ni with respect to Cu decreased with increasing fluence. They used a standard brass sample and a quadrupled Nd:YAG laser (λ = 266 nm) for ablation. Figg and Kahr[15] applied ns-laser pulses of different wavelengths to a glass sample. In their experiment they changed the laser fluence by varying the distance between the focus point and the sample surface. They reported very strong elemental fractionation of several elements, which was also dependent on the laser wavelength. The results of

[a]*ISAS – Institute for Analytical Sciences at the Technical University of Dortmund, Germany. E-mail: garcia@isas.de; lindner@isas.de; a.vonbohlen@isas.de; niemax@isas.de*
[b]*Institute of Physics, Zagreb, Croatia. E-mail: vadla@ifs.hr*

Mao *et al.*[16] on fractionation of Zn and Cu at ns-LA of brass supported the earlier findings of Cromwell and Arrowsmith.[14] At low fluence of a Nd:YAG laser (λ = 1.06 μm) more Zn than Cu was removed from the sample. Chen,[17] who studied elemental fractionation of glass and fused silicate rock samples by ns-LA-ICP-MS (λ = 266 nm) found a dependence of fractionation not only on fluence but also on time. For the first time, a correlation between elemental fractionation and the ionization energies of the elements was postulated. However, it was also shown in ref. 12–17 that the fractionation problem can be avoided or reduced when laser fluences well above the ablation thresholds of the samples were applied.

The present paper will show that the elemental composition of the particle mass ablated by fs-laser pulses changes from shot to shot at the beginning of ablation and becomes constant after a number of shots. Such measurements with successive single laser shots at pulse rates of 1 Hz or higher are possible if ablation cells with very short times for *complete* particle washout are used. This favourable condition is provided by the sampling tube ablation cell described in ref. 7 and 10. Any cell with larger cross-section than the transport tube might produce ICP-MS signals of comparable half-width at the same gas flow conditions but will need a much longer time for *complete* washout of all particles.

It will be demonstrated that the asymptotic, constant element ratios measured at high shot numbers are independent of laser fluence and the samples probed, but are proportional to the actual elemental concentration ratios in the samples. This is the basis for stoichiometric sampling and non-matrix-matched calibration as demonstrated in ref. 11 and 12. The complementary elemental enrichments or depletions in the bottom layers of the laser craters are also demonstrated. The element ratios in the ablated aerosol masses were measured shot by shot by applying ICP-MS, while scanning electron microscopy-energy dispersive X-ray spectroscopy (SEM-EDX) was used to determine elemental changes in the bottom layers of the laser craters. The averaged thickness of the modified layer could be estimated from the X-ray emission by applying different electron energies, *i.e.* different electron penetration depths, and through Monte-Carlo calculations of the motion of electrons and the paths of X-ray photon in the sample.[18–21]

Furthermore, it will be shown that there seems to be a correlation between preferential elemental ablation and the ionization energies of the elements as suggested already by Chen,[17] *i.e.*, elements with lower ionization energy than others were enriched in the mass ablated in almost all cases, while elements with comparable ionization energies do not show significant fractionation. These findings reveal that the theory of laser ablation[22–25] needs refinement.

Experimental

Solid samples were placed in an ablation cell and probed under an argon atmosphere by single shots of a fs-laser (Hurricane, Spectra Physics) providing 120 fs pulses at λ = 795 nm and up to 750 μJ of pulse power. The laser beam had a Gaussian shape, *i.e.*, no intensity homogenization was made. In order to be able to measure elemental fractionation in successive shots, the sampling tube ablation cell[7,10] was used to provide a very short time for *complete* particle washout. The data were taken at five different positions of the samples and averaged for each shot. Pulse energies between 50 and 350 μJ were applied and the fluence on the sample surface was varied either by changing the focus position of the focussing lens relative to the surface or by tuning the laser power. Not more than 32 shots were applied in order to avoid drilling of deep craters and alteration of the fluence delivered to the crater bottoms. The focus position was determined experimentally from the crater diameters produced with stepwise defocused lens positions (step width: 0.3 mm). The error of the experimentally determined focal length is 0.1–0.2 mm. The fluences were calculated by applying the $1/e^2$ criterion to the Gaussian beam (see, *e.g.* ref. 5).

However, in all cases care was taken to avoid a plasma breakdown in the gas above the sample. Plasma breakdown can be observed if the laser beam is tightly focussed onto the sample in an Ar atmosphere. The plasma expansion modifies the spatial particle distribution after the laser shots[13] and leads to particle losses on the sample surface.[8]

The particles were transported by He (flow: 1.3 l min^{-1}) or Ar (flow: 0.8 l min^{-1}) from the sampling tube through a flexible tube to a commercial ICP-MS instrument for relative element ion ratio measurements. For proper operation of the ICP an additional Ar flow (1.55 or 0.8 l min^{-1} for He or Ar ablation, respectively) was added before the plasma torch. Since fs-laser generated particles are sufficiently small,[5,6] they are fully atomized in the hot ICP. Therefore, the isotopic element ratios measured by mass spectroscopy are proportional to the element ratios in the mass ablated taking into account the transport efficiency in fs-LA, which is near unity.[7,8] However, care has to be taken that the particle load in the plasma is not too large since mass dependent influences on the plasma parameters should be excluded. The commercial quadrupole ICP-MS instrument (Agilent 4500) was tuned with a frequency of ~200 Hz between the isotopic components of interest. The integration time for each element was between 2 and 4 ms depending on the strengths of the transient ion signals (total length: <1 s). The measured signals were summed up for each element and then rationed. Additional information about the used ICPMS settings can be found in ref. 7.

In order to get complementary information on the element ratio changes on a shot-to-shot basis, the elemental composition of the bottom layer of the laser crater was measured by an EDX-system (Quantax 400, Bruker) attached to a high resolution scanning electron microscope (Quanta 200F by FEI). For these measurements laser craters made with different numbers of shots were analyzed either by SEM-EDX line-scan or pointwise. The SEM-EDX-instrument was operated at low acceleration voltage (1.5 to 11 kV, tunable in 100 V steps) for the inspection of the laser craters. Each crater was analyzed with different electron energies to get access to the required information. The electron penetration depths, the motion of the electrons and the absorption of X-ray photons in the samples were calculated using a Monte-Carlo freeware simulation program.[26]

Samples

Conducting and semi-conducting samples (Cu–Zn, Ni–Fe, Ag–Cu, Pb–Sb, Cr–Fe, GaAs) containing two major elements each

Table 1 Analysed samples, element concentrations and ratios, isotopes measured by fs-LA-ICP-MS and the first ionization potential of the elements

Sample	Element concentration	Element ratios	Analysed isotopes	1st Ionization potential/eV
Brass Naval 1107	Cu: 61.2 %; Zn: 37,3 %	Cu/Zn: 1,64	^{65}Cu; ^{66}Zn ^{65}Cu; ^{67}Zn	Cu: 7.73; Zn: 9.40
Ag–Cu	Ag: 40 %; Cu: 60 %	Ag/Cu: 0.67	^{107}Ag; ^{65}Cu	Ag: 7.58; Cu: 7.73
Ni–Fe	Ni: 50 %; Fe: 50 %	Ni/Fe: 1.00	^{62}Ni; ^{57}Fe	Ni: 7,64; Fe: 7.87
Cr–Fe	Cr: 41.1 %; Fe: 58.9 %	Cr/Fe: 0.7	^{53}Cr; ^{57}Fe	Cr: 6.77; Fe: 7.87
Pb–Sb	Pb: 54.8 %; Sb: 45.2 %	Pb/Sb: 1.21	^{204}Pb; ^{123}Sb	Pb: 7.42; Sb: 8.64
GaAs	Ga: 51.2 %; As: 48.2 %	Ga/As: 1.08	^{71}Ga; ^{75}As	Ga: 5.99; As: 9.81
NIST 610 glass	Cu: 444 ppm; Zn: 433 ppm	Cu/Zn: 1.03	^{65}Cu; ^{66}Zn	Cu: 7.73; Zn: 9.40
NIST 1412 glass	Cd: 3.83 %; Ba: 4.18 %	Cd/Ba: 0.92	^{111}Cd; ^{137}Ba	Cd: 8.99; Ba: 5.21
	Pb: 4.08 %; Zn: 3.60 %	Pb/Zn: 1.13	^{208}Pb; ^{66}Zn	Pb: 7.42; Zn: 9.40
	Al: 3.98 %; Si: 19.81 %	Al/Si: 0.20	^{27}Al; ^{29}Si	Al: 5.99; Si: 8.15
	Sr: 3.85 %; Zn: 3.60 %	Sr/Zn: 1.07	^{88}Sr; ^{66}Zn	Sr: 5.70; Zn: 9.40

with concentration ratios of the order of 1 : 1 were used, as well as standard glass (NIST 610 and NIST 1412) including several elements with concentrations between ~400 ppm and ~20 %, respectively. All samples, except GaAs (fresh wafer) were polished with a diamond suspension and washed by methanol or de-ionized water before ablation. Brass and glass samples were ablated in helium, while argon was applied as ablation gas for all other samples. Detailed information on the element concentrations in the samples, as well as the measured isotopes and the first ionization potential of the analyte elements, are included in Table 1.

Results

Fractionation of Cu and Zn from brass and glass samples

A matrix which was and still is used for demonstration of element fractionation is brass. Brass has a low melting point (~910 °C) and is made of two elements with very different thermal properties (the vapour pressures differ by many orders of magnitude). Applying ns-LA with low laser fluences, there is a strong preferential ablation of Zn.[14,16] This situation reverses if brass is ablated by ultra-short laser pulses. Fig. 1 shows the ratio of the averaged integrated ^{65}Cu and ^{67}Zn signals for the first shots on five fresh positions applying three different fluences. It can be seen that initially there is preferential sputtering of Cu in fs-LA of brass. This effect is stronger when low laser fluences are applied. However, at sufficiently high shot numbers the ratio is independent of the fluence within the limits of experimental uncertainty (see Fig. 1). It has to be stressed that element ratios of successive single shots are measured in the present experiment while fractionation effects are usually measured at high pulse frequency, *e.g.* 10–20 Hz, in ablation cells where the particle masses of successive shots are mixed. Therefore, fractionation effects as shown in Fig. 1 are temporally smeared.

In further measurements the fractionation of Cu and Zn from the NIST 610 glass sample was investigated by fs-LA-ICP-MS. The experimental results are shown in Fig. 2. Here the more abundant ^{66}Zn isotope was measured because of sensitivity reasons (low element concentrations in the sample). Qualitatively there is a similar trend of preferential ablation as with brass (see inset), Cu being enriched in the mass sampled with the first shots. This effect is particularly strong if laser sampling is made near to the ablation threshold. Note that Cu is about 10-fold enhanced in the first shot with 3.1 J cm^{-2} in comparison to shot numbers beyond 20. This effect is smaller at higher fluences. For example, already the second shot at 89.5 J cm^{-2} gives a mass

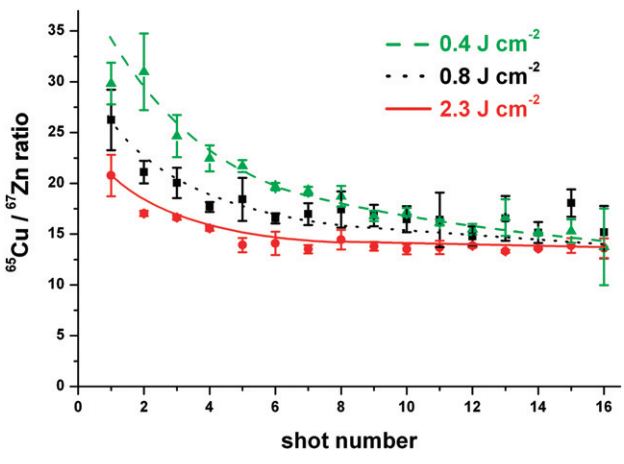

Fig. 1 ^{65}Cu/^{67}Zn ratios measured in brass by successive single fs-laser shots of different fluences and ICP-MS detection. The dashed, dotted and solid lines do not present mathematical fits; they are manually drawn to guide the eye.

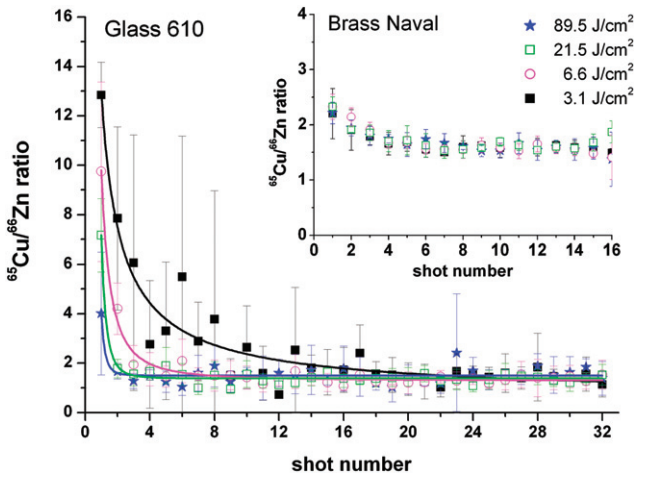

Fig. 2 ^{65}Cu/^{66}Zn ratios measured by successive single fs-laser shots and ICP-MS in the Naval brass and 610 glass samples at different laser fluences. The curves do not present results of mathematical fits to the respective data points; they are manually drawn to guide the eye.

ratio which does not change at higher shot numbers. The similar fractionation of Cu and Zn in brass and glass is a first hint that elemental fractionation is in first order qualitatively independent of the matrix.

There are two results which are important for fs-LA-ICP-MS: (i) within their mutual error bars, the asymptotic Cu/Zn ratios are independent of the laser fluence at sufficiently high shot number for different matrices and concentrations, and (ii) the asymptotic ratios measured in brass and glass reflect the relative Cu/Zn ratios in both samples, which is 1.58 for brass to glass (see Table 1). This means that we have stoichiometric ablation at sufficiently high shot number, the pre-condition for non-matrix-matched calibration in fs-LA-ICP spectrometry demonstrated recently.[11,12]

The fractionation effect obtained with the NIST 610 standard glass agrees qualitatively well with the Cu and Zn data obtained recently with the same sample (see ref. 12,13). In both papers the elemental fractionation of Cu and Zn was also found to be dependent on the fluence. However, the measurements were made with ablation cells of somewhat larger volume where the information on the concentration ratio in the particles from different shots is mixed. Nevertheless, it was shown before that high fluences have to be applied to approach stoichiometric ablation, in agreement with the results of the present experiment.

Fractionation measured with binary samples

In order to find correlations between elements and fractional ablation, five binary samples (GaAs, Ag–Cu, Cr–Fe, Ni–Fe, Pb–Sb) were investigated in addition to Cu–Zn. The fs-LA-ICP-MS results derived from the first 16 shots with fluences of 0.4 and 2.3 J cm^{-2} are displayed in Fig. 3.† Fractional element ablation can be observed for all samples in the first shots, and the effect is more pronounced at lower fluence. All element ratios approach a constant value at higher shot number which is independent of fluence within the mutual experimental errors as found for the Cu/Zn ratio by fs-LA-ICP-MS.

Fractionation studies using the NIST 1412 glass sample

Elemental fractionation measurements of Al, Ba, Cd, Pb, Si, Sr, and Zn in the NIST 1412 glass applying a low fluence (3.1 J cm^{-2}) revealed qualitatively the same trend as observed with the binary metallic and semiconductor samples. For most element ratios the fractionation effect in the first shots was small. The data are not given in a separate figure since the error bars (up to about 30%) were often larger than the fractionation effect, although the element concentrations were much higher than in the NIST 610 glass. We suggest that the large uncertainties are due to element inhomogeneities in the 1412 glass sample.

Enrichment and depletion of elements in the laser craters

Enrichments or depletion of elements should be observable in the laser crater if there is preferential elemental ablation by fs-laser pulses. Therefore, the craters of the brass and the GaAs samples,

† The Ag/Cu ratio measured at 2.3 J cm^{-2} has not been included in Fig. 3 since the ratio monotonically increased at higher shot number due to an unknown effect.

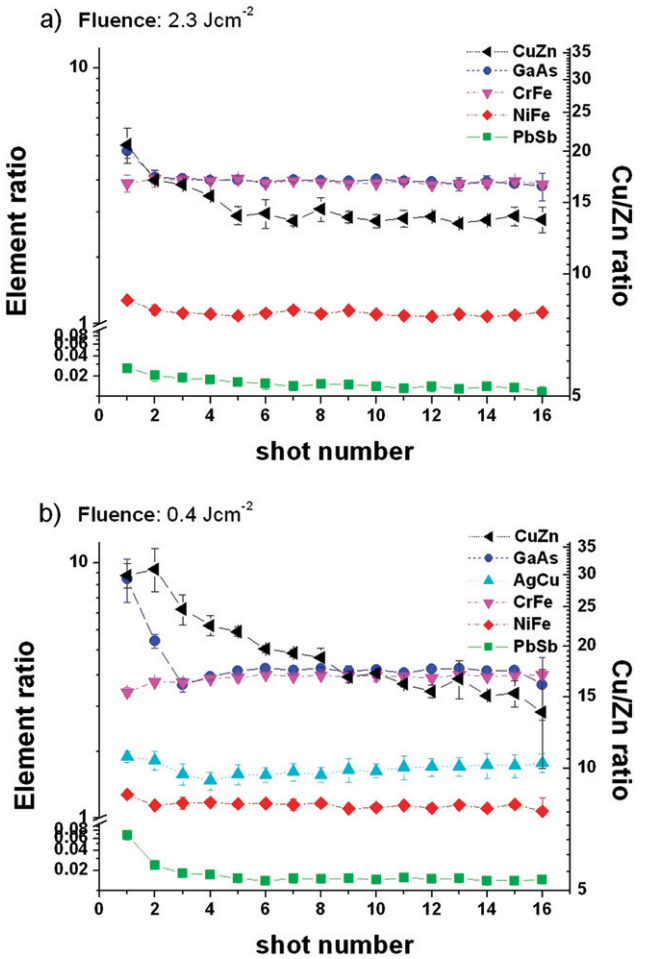

Fig. 3 Logarithmic plot of the element ratios measured in different binary samples by single successive fs-laser shots of different fluence (a: 2.3 J cm^{-2}, b: 0.4 J cm^{-2}) and ICP-MS. There is a separate logarithmic ordinate for the Cu/Zn ratio at the right side of the figure.

which both showed significant fractionation (see Fig. 3), were analysed by SEM-EDX. The path of the scan is shown as a white line in Fig. 4a, which is a SEM picture of a brass crater produced by 16 laser shots with 0.8 J cm^{-2}. The relative concentrations of Zn and Cu are given by the upper two signals in Fig. 4b. The lower two traces show the relative concentration of C and O. Obviously, C and O are responsible for the dark halo around the crater (see Fig. 4a). Quantitative EDX measurements with different electron energies (see below) gave a maximum thickness of the C–O layer of about 37 nm after 16 shots (Fig. 4c). Both elements stick to the surface due to reactions between surface and gaseous compounds in Ar during the time when the region around the crater is hot. The higher O concentration in the halo around the crater could be due to surface oxidation, probably by traces of water in the cell gas. The relatively thick C layer is surprising since the Ar gas used has a relatively high degree of purity (99.99 %).

The enrichment of Zn and the depletion of Cu in the crater can already be taken from the raw data shown in Fig. 4b. The averaged Zn and Cu concentrations and the average thickness of the modified layers were derived from EDX measurements with different electron energies, as mentioned above. It was assumed

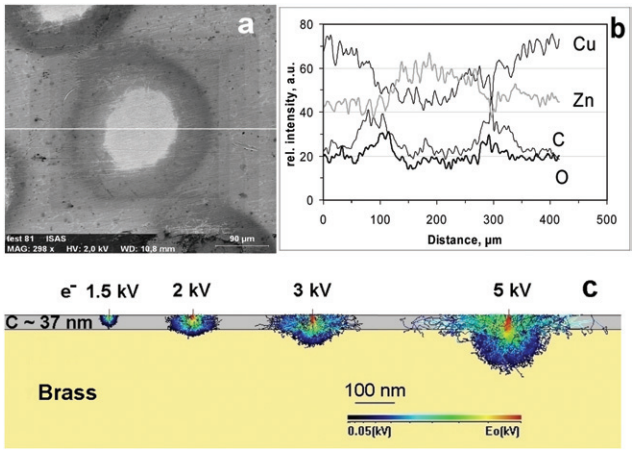

Fig. 4 (a) SEM picture of a brass crater obtained with 16 femtosecond laser shots (fluence: 0.8 J cm^{-2}). (b) Relative Cu, Zn, C and O signals measured by EDX across the crater (the path of scan is shown as white line in the SEM picture). (c) Monte-Carlo simulations of electron paths in the sample for evaluation of the C-layer thickness of the dark halo around the crater (see SEM picture).

that the affected layers at the bottom of the craters were even and that there was no gradient of the Zn/Cu concentration ratio in the layers. As shown in Fig. 4c for a C-layer, the electron penetration depths can be estimated by Monte-Carlo calculations taking into account the matrix composition. The X-ray emission of the Zn and Cu K_α lines is partly generated in the modified layer and with increasing electron penetration depth in the bulk below. The element concentration in the affected layer as well as the average thickness of the affected layer can be evaluated by interpolation from this procedure.[18–21]

Fig. 5 shows the Cu and Zn concentrations measured with two different electron energies (3 and 5 keV) in different positions outside and inside the brass craters produced by 2, 8 and 16 laser shots. The data points were obtained by scanning the electron beam over small circular areas with 50 µm diameter and integrating the X-ray line intensities. Significant enrichments of Zn could already be seen after two laser shots (a). The process of Zn enrichment was continued from shot to shot and stabilized after the seventh shot. Note that the ratios measured in the centres of the craters made by 8 (b) and 16 shots (c) are the same within the limit of experimental uncertainty. Only the area of the modified layer is a little larger in the 16-shot crater. However, the area did not further increase with higher shot number. These findings correlate with the Cu/Zn ratio measurements at 0.8 J cm^{-2} shown in Fig. 1. Note that the Cu/Zn ratio was nearly independent of the laser shot number for shots larger than 8.

It is interesting that the average thickness of the modified brass layer derived from measurements with different electron energies is on the order of 30–50 nm. This is much smaller than the roughness of the crater bottom. Fig. 6 displays a SEM picture of the central region of a 16-shot laser crater. We see a "frozen" melt layer with ascending droplet-shaped material. The surface roughness for 16 shots at 0.8 J cm^{-2} can be estimated to be on the order of 1 µm. The roughness increases if more shots or shots with higher fluences are applied. Additional EDX measurement of ascending droplets and the bottom region marked by circles in

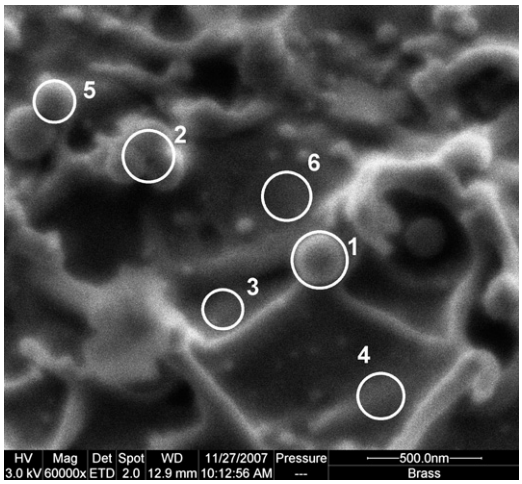

Fig. 6 Magnified SEM picture of the crater bottom produced with 16 fs laser shots (fluence: 0.8 J cm^{-2}) on a brass sample. The circles mark very small areas where EDX measurements of Zn and Cu were made. The circles marked 1, 2 and 5 comprise three uprising re-solidified droplets, while those marked 3, 4 and 6 are areas at the bottom of the crater.

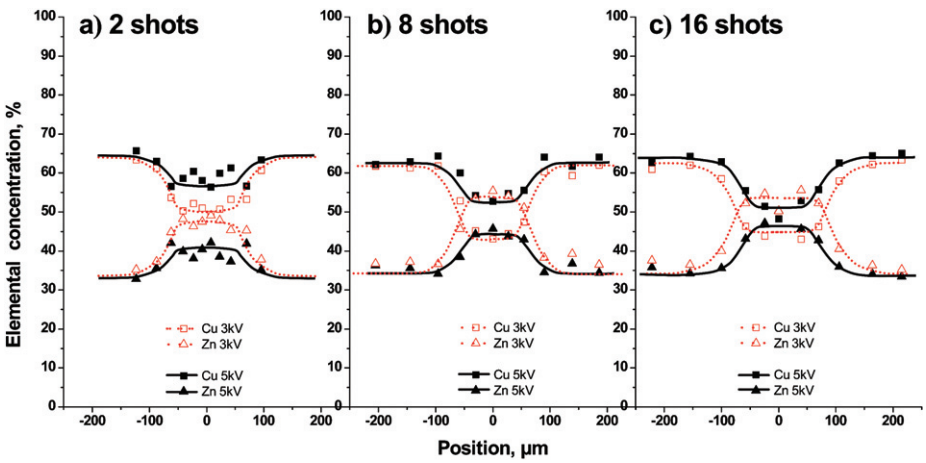

Fig. 5 Zn and Cu concentrations measured by EDX with 3 and 5 keV electrons in different positions inside and outside laser craters produced by 2, 8 and 16 fs laser shots on the Naval brass sample. Laser fluence: 0.8 J cm^{-2}.

Fig. 6 revealed significant differences in the Cu/Zn ratio. While the Zn and Cu concentrations in the bottom layers were in rough agreement with the averaged data presented in Fig. 5c, the Cu/Zn concentration ratio in the "frozen" droplets was on the order of 2, which is higher than in the bulk (1.64, see Table 1).

EDX measurements of the GaAs laser crater yielded, as expected from the fractionation studies displayed in Fig. 3, significant As enrichments in the averaged bottom layers of the craters. The averaged layer thickness was estimated to be ~50 nm. The roughness of the crater bottom and the "frozen" droplets were both much smaller than in brass. As found around the brass craters, there was also a halo of C and O around the GaAs craters. However, the amount of C was smaller and the relative amount of O higher than in the brass case.

Discussion

In order to understand the experimental findings on elemental fractionation, let us assume that we have a *homogeneous* binary sample (elements: X and Y) and a laser with *flat-top profile* of *low fluence*. Furthermore, we assume that the two elements of the sample have different ablation probabilities (a possible reason for such a difference will be discussed below), for example, by a factor of two, while the concentration ratio in the bulk is chosen to be one. At low laser fluence conditions, the first shot will remove two times more mass of element X than of element Y. Thus the element Y is enriched in the upper layer of the laser crater. The next shot removes mass with a smaller X/Y ratio than the first shot since the element X was somewhat depleted in the upper layer after the first shot. After a sufficiently large number of shots the X/Y ratio in the mass ablated will be theoretically one which represents the concentration ratio in the bulk, although the concentration ratio in the modified layer is now 0.5 in our simple picture. Note that stoichiometric ablation will always occur independently of differences in the ablation probability at low, spatially constant laser fluence after a sufficiently large number of shots. However, no fractionation would be observed if the ablation probability of the elements is the same.

Here, it has to be mentioned that fractionation, elemental depletion and finally stoichiometric sampling by laser ablation is similar to preferential elemental sputtering observed in glow discharge (GD) analysis of solid samples. However, preferential sputtering of Zn has been measured at the beginning of GD analysis of brass,[27] while Cu was the preferred element in fs-LA.

If the flat-top laser beam is delivering *high fluence* onto the homogeneous sample with a fresh surface, the first shot would remove a much thicker layer (many atomic layers) with the bulk composition and a comparable smaller mass with an excess of element X. Theoretically the element ratio in the small mass fraction should be two, since the laser leaves the complementary mass as a resolidified layer in the crater with a X/Y concentration ratio of 0.5, the same as with low fluence after many shots. The following high-fluence shots will ablate stoichiometrically, since the total ablated mass consists of the mass of the modified upper layer (X/Y = 0.5), the bulk (X/Y = 1) and an again smaller mass fraction with X/Y = 2, complementary to the newly modified upper layer of the sample surface. It means that in our simple theoretical case fractionation will be observed only in the first shot if high fluences are applied.

In fact, fractionation can always be observed experimentally in the first shot if two elements have different ablation properties. Note that fractionation from the brass sample could not be avoided even by applying very high fluences (see inset of Fig. 2). The reason why the second and also the third shot do not ablate completely stoichiometrically at high fluence is the Gaussian beam profile. There might be stoichiometric ablation in the center of the crater but non-stoichiometric ablation near the crater rim because of the lower spatial fluence of the Gaussian beam in that region. At higher shot number the total area of stoichiometric ablation gets larger and the mass removed non-stoichiometrically near the crater rim can be neglected. This means that the crater area with stoichiometric ablation covers, independent of the spatially removed mass, most of the crater as shown in Fig. 5. However, it has to be pointed out again that the crater bottom is not even and that there are very small areas, the regions with "frozen" uprising droplet-shaped melt (see Fig. 6), where the elemental composition is obviously predominantly affected by thermal fractionation. The depletion of Zn found in the "frozen" droplets well above the crater bottom is similar to that found for the incompletely atomized bigger brass particles collected in a recent investigation of size distribution and elemental composition of particles produced by fs-LA of brass.[5] Furthermore, the enrichment of Zn in the 30–50 nm bottom layers is expected to change with depth, approaching the concentration of the bulk.

The elemental fractionation by successive laser shots can be given by a simple theoretical model. As above, we assume that we have a *homogeneous* binary sample (elements: X and Y with concentrations $N_X(0)$ and $N_Y(0)$ (cm^{-3}) with a ratio $R_0 = N_X(0)/N_Y(0)$) and a laser with *flat-top profile* of fluence F (J cm^{-2}). Furthermore, we assume that the fs-laser pulse energy is homogeneously stored in the volume SD, where D is the penetration depth of the laser and S is the cross-sectional area of the laser beam. The stored energy causes the ablation, which can be described by $dZ_i/dF = -a_i Z_i$. Here, the $Z_i = SDN_i$ are the number of atoms in the volume SD, and a_i (J^{-1} cm^2) are defined as ablation rates for the particular elements i = X, Y. Then, the element ratio in the mass ablated by the first laser shot is

$$R_{XY}(1) = \frac{1 - \exp(-a_X F)}{1 - \exp(-a_Y F)} R_0 \qquad (1)$$

and the remaining number of atoms $Z'_X = Z_X(0)\exp(-a_X F)$ and $Z'_Y = Z_Y(0)\exp(-a_Y F)$ will be re-solidified in the upper layer (thickness: d_1) of the flat laser crater. At low laser fluence conditions ($a_i F \ll 1$), the first shot will remove the material with concentration ratio $R_{XY}(1) \approx (a_X/a_Y)R_0$. Obviously, no fractionation would be observed if the ablation rates of the elements are the same. In case of high laser fluence ($a_i F \gg 1$), the ratio $R_{XY}(1)$ is equal to the stoichiometric ratio R_0.

The second laser shot with the same laser penetration depth D interacts with the modified layer of thickness d_1 and the bulk layer below having a thickness ($D - d_1$). Here, we assume that the total concentration $N'_X + N'_Y$ in the modified layer is equal to the total concentration $N_X(0) + N_Y(0)$ in the bulk, *i.e.* $(Z'_X + Z'_Y)/d_1 = (Z_X(0) + Z_Y(0))/D$. Then, the numbers of atoms $Z_X(1)$ and $Z_Y(1)$ in the interacting volume SD can be expressed in terms of R_0, a_X, a_Y and F. The iterative application of this simple

model yields the following recursive expression for the element ratio in the mass removed by the nth laser shot:

$$R_{XY}(n) = \frac{1-\exp(-a_X F)}{1-\exp(-a_Y F)} \frac{A_n}{B_n} R_0 \quad (2)$$

where

$$A_n = 1 + A_{n-1}\exp(-a_X F) - \frac{A_{n-1} R_0 \exp(-a_X F) + B_{n-1}\exp(-a_Y F)}{R_0 + 1}$$

and

$$B_n = 1 + B_{n-1}\exp(-a_Y F) - \frac{A_{n-1} R_0 \exp(-a_X F) + B_{n-1}\exp(-a_Y F)}{R_0 + 1} \quad (3)$$

with $A_1 = 1$ and $B_1 = 1$. Numerical analysis shows that even for the low fluence case the ratio $R_{XY}(n)$ approaches R_0 for large shot numbers n. This is consistent with the experimental findings, which show that stoichiometric ablation will always occur independently of differences in the ablation probability after a sufficiently large number of shots.

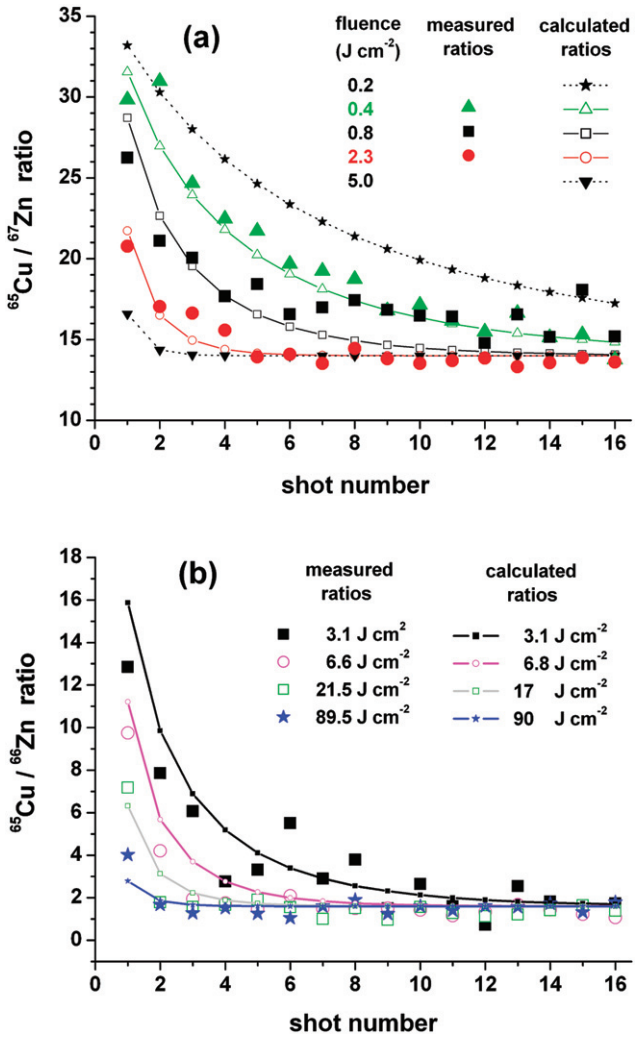

Fig. 7 (a) Theoretical fits of the fractionation formula (eqn (2)) for the measured Cu/Zn ratios to the experimental data presented in Fig. 1. The ratios plotted with the symbols ★ and ▼ are extrapolations for the fluences 0.2 and 5.0 J cm^{-2}, respectively. (b) Theoretical fits of the fractionation formula to the Cu/Zn ratios measured in glass (see Fig. 2).

It is interesting to show that the very simple model above can describe the experimental observations surprisingly well. Fig. 7a shows fits of the fractionation formula (eqn (2)) to the experimental data presented in Fig. 1. Only the experimental R_0 and the data obtained at a fluence of 0.4 J cm^{-2} were taken into account to derive the ablation rates a_X and a_Y. The calculated ratios for the experimental fluences of 0.8 and 2.3 are in good agreement with the measured data. The theoretical data for 0.2 and 5 J cm^{-2} are presented to show the differences in elemental fractionation if the laser fluence was to be lowered or increased, respectively. The agreement between simple theory and experiment is also good if we fit eqn (2) to the Zn/Cu ratios measured in the NIST 610 glass sample (see Fig. 7b). Here, the theoretical data were adjusted to the data measured at 3.1 J cm^{-2}. The fluences derived from the best fit to the other experimental data are in surprisingly good agreement with the fluences calculated from the 1/e^2 criteria and the measured defocusing. The uncertainties of the relative fluence is in particular large if measurements are performed with a focussed beam (fluence: 89.5 J cm^{-2}) or with 0.5 mm defocusing (21.5 J cm^{-2}), since the error in the focal length determination was 0.1–0.2 mm, as mentioned in the Experimental section of this paper.

One of the major reasons for different elemental ablation probabilities, *i.e.* elemental fraction in laser ablation, might be connected with the ionization energies of the elements, as already suggested by Chen.[17] To support this statement, the element ratios in Figs. 1–3 are plotted in such a way that the elements with the corresponding lower ionization limit stands always in the numerator of the ratio (see ionization energies in Table 1). There is a general trend that the element with lower ionization energy is preferentially ablated in the first shots independent of its respective thermal volatility. The effect is pronounced for Cu–Zn, GaAs and Pb–Sb, and weaker for Ni–Fe and Ag–Cu where the ionization energy differences are smaller. The only exception is the binary sample Cr–Fe where small but significant preferential ablation of Fe was recorded by LA-ICP-MS in the first shots (Fig. 3). Although the ionization energies differ by 1.1 eV, the Cr/Fe ratio is slightly lower than the asymptotic limit increasing with the first few shots.

Preferential ablation of elements with low ionization limits might be a sign for a major influence of Coulomb interaction in the fractionation mechanism. There is a debate on the influence of Coulomb interaction in fs-LA (see, *e.g.* ref. 28 and references therein). Coulomb repulsion of ions ('Coulomb explosion') seems to be a major force in fs-LA of non-conducting samples, since high velocities of atomic ions have been measured after interaction of fs-laser pulses with the material.[27] However, in the same paper the influence of Coulomb interaction was regarded as minor if conducting samples are ablated. On the other hand, Albert *et al.*[29] measured fast titanium ions generated by fs-LA of a pure titanium metal sample, indicating that the Coulomb interaction of the target ions must also be taken into account for conducting samples.

In fs-LA free and bound electrons in the solid are excited and rapidly heated in the photon absorption layer, *i.e.*, a kind of metastable, high-density plasma with extremely hot electrons and relative cold ions and atoms is formed in a time scale of <1 ps, as discussed in, for example, ref. 22. The ions and atoms are so close together that immediate exchange of electrons and

excitation energy can be expected between ion and atoms on the one hand, and between element ions in different ionization stages on the other. Therefore, it is conceivable that the ion concentration of elements with lower ionization energy is higher than of elements with higher ionization potential before the heavy particles are heated by electron collisions. In the next phase, the kinetic energy of the heavy plasma particles, the ions and atoms, rises rapidly due to collisions with hot electrons presenting the thermal contribution to the propagation of sample mass in the ablation process. Note that the energy of the electrons is so high that even inner shell electrons of atoms are kicked out by collisions followed by inner shell transitions, *i.e.* very short pulse of hard X-ray radiation.[30] On the other hand, there are the strong Coulomb repulsion forces between nearby element ions in the very dense plasma at the very beginning that make an early contribution to the kinetic energy of the heavy plasma particles in the expansion process. It is possible that this early ion-dependent contribution results in a spatial de-mixing of elements if the ion concentrations of the elements are different. A fraction of the affected matter can be found as re-solidified layer at the bottom of the craters, which show enrichment or depletion of elements due to former spatial de-mixing driven by Coulomb repulsion in the early plasma state.

The suggestion that fractional ablation of elements is connected with the ionization energy is also supported by the fs-LA-ICP-MS measurements of Pb/U and U/Th in glass of Koch *et al.*,[13] who reported a growing Pb/U ratio with increasing fluence but almost no fractionation of the U/Th ratio. Note that U and Th have almost the same ionization energies (U: 6.2 eV, Th: 6.3 eV), while the ionization energy of Pb (7.5 eV) is higher than of U. Furthermore, the elemental fractionations found in ns-LA (see, *e.g.* ref. 15) also support the assumption that different ionization energies might be responsible for preferential ablation in the first shots, although an influence of thermal fractionation cannot be excluded during the long interaction time of the laser with the laser-induced plasma above the crater, in particular when the boiling points of elements are very different. Brass, with many orders of magnitude difference between the vapour pressures of Zn and Cu, is such a case. This is probably the reason why Crowell and Arrowsmith[14] and Mao *et al.*[16] found preferential ablation of Zn at low fluences, different from the finding in ref. 12,13 and in the present paper.

Conclusion

Elemental fractionation in fs-LA has been observed at the first laser shots on a fresh sample. The elemental fractionation effects were strong when laser fluences near to the ablation threshold of the samples were applied. The measured element ratios were found to approach asymptotic values at higher shot number that were independent of laser fluence. These asymptotic ratios represent the stoichiometric ratios of elements in the solid sample within the mutual experimental uncertainties, as shown for the Cu/Zn ratios in brass and glass. These findings support the recent non-matrix-matched calibration studies on brass, aluminium and glass by fs-LA-ICP-OES/MS.[11,12]

It was hypothesized that a major reason for elemental fractionation in fs-LA is due to different ionization energies of the elements and to Coulomb interaction of the ions in the plasma state of matter during the ablation process. However, it cannot be excluded that thermal evaporation, particularly of volatile elements, may obscure the ionization energy dependent elemental fractionation effect. Elemental fractionation effects have not yet been taken into account in theoretical modelling of laser ablation.[22–25] In this regard theory needs refinement, in particular since elemental fractionation is also an important issue in several other application fields of LA, such as surface modification of materials by laser interaction, chemical vapour deposition with lasers, and geochemical dating of rocks.

Finally, we want to point out that fractional ablation has not only to be taken into account in LA-ICP-MS but also in laser-induced breakdown spectroscopy (LIBS),[31] where often very different intensities of the elements are observed in the first shots on a fresh sample. Therefore, these early LIBS data are usually discarded from the analysis. For fs-LA-ICP-MS analysis of homogeneous samples, elemental fractionation can be taken into account if a number of shots can be applied. However, the effect will cause errors if inhomogeneous samples are analysed or in-depth profiling of thin films with low fluence (for high depth resolution) is performed.

Acknowledgements

Project funding by the Deutsche Forschungsgemeinschaft is gratefully acknowledged. The authors also thank the Ministry of Innovation, Science, Research and Technology of the state Northrhine-Westphalia and the Ministry of Education and Research of the Federal Republic of Germany for general support.

References

1 A. L. Gray, *Analyst*, 1985, **110**, 551.
2 A. Montaser, *Inductively Coupled Plasma Mass Spectrometry*, Wiley-VCH, New York, 1998.
3 R. E. Russo, X. Mao, H. Liu, J. Gonzales and S. S. Mao, *Talanta*, 2002, **57**, 425.
4 D. Günther and B. Hattendorf, *TrAC, Trends Anal. Chem.*, 2005, **24**, 255.
5 J. Koch, A. von Bohlen, R. Hergenröder and K. Niemax, *J. Anal. At. Spectrom.*, 2004, **19**, 267.
6 J. Koch, H. Lindner, A. von Bohlen, R. Hergenröder and K. Niemax, *J. Anal. At. Spectrom.*, 2005, **20**, 901.
7 C. C. Garcia, H. Lindner and K. Niemax, *Spectrochim. Acta, Part B*, 2007, **62**, 13.
8 C. C. Garcia, M. Wälle, H. Lindner, J. Koch, K. Niemax and D. Günther, *Spectrochim. Acta, Part B*, 2008, **63**, DOI: 10.1016/j.sab.2007.11.017.
9 P. A. Baron and K. Willeke, *Aerosol Measurements: Principles, Techniques and Applications*, John Wiley & Sons, New York, 2001.
10 D. Autrique, A. Bogaerts, H. Lindner, C. C. Garcia and K. Niemax, *Spectrochim. Acta, Part B*, 2008, **63**, DOI: 10.1016/j.sab.2007.11.032.
11 Q. Z. Bian, J. Koch, H. Lindner, H. Berndt, R. Hergenröder and K. Niemax, *J. Anal. At. Spectrom.*, 2005, **20**, 736.
12 Q. Z. Bian, C. C. Garcia, J. Koch and K. Niemax, *J. Anal. At. Spectrom.*, 2006, **21**, 187.
13 J. Koch, M. Wälle, J. Pisonero and D. Günther, *J. Anal. At. Spectrom.*, 2006, **21**, 942.
14 E. F. Cromwell and P. Arrowsmith, *Anal. Chem.*, 1995, **67**, 131.
15 D. Figg and M. S. Kahr, *Appl. Spectrosc.*, 1997, **51**, 1185.
16 X. L. Mao, A. C. Ciocan and R. E. Russo, *Appl. Spectrosc.*, 1998, **52**, 913.
17 Z. Chen, *J. Anal. At. Spectrom.*, 1999, **14**, 1823.
18 D. F. Kyser and K. Murata, *IBM J. Res. Dev.*, 1974, **18**, 352.
19 Y. Nakagawa, K. Murata and K. Takeuchi, *J. Phys. D: Appl. Phys.*, 1993, **26**, 1764.

20 M. Yasuda, S. Yamauchi, H. Kawata and K. Murata, *J. Appl. Phys.*, 2002, **92**, 3404.
21 R. Butz and H. Wagner, *Phys. Status Solidi A*, 2006, **3**, 325.
22 P. Gibbon, *Short Pulse Laser Interaction with Matter – An Introduction*, Imperial College Press, London, 2005.
23 S. I. Anisimov and B. S. Luk'yanchuk, *Phys.–Usp.*, 2002, **45**, 293.
24 D. Bäuerle, *Laser Processing and Chemistry*, Springer, New York, 2000.
25 *Laser Ablation and its Applications (Springer Series in Optical Sciences)*, ed. C. R. Phipps, Springer, New York, 2006.
26 D. C. Joy, *Monte-Carlo Simulation V2.37 (Bulk with Thin Film)*, freeware available from. E-mail: kanda.kimio@naku.hitachi.hitec.com.
27 B. V. King, R. Payling, in *Glow Discharge Optical Emission Spectrometry*, ed. R. Payling, D. Jones and A. Bengtson, John Wiley, New York, 2000, p. 273.
28 R. Stoian, A. Rosenfeld, D. Ashkenasi, I. V. Hertel, N. M. Bulgakova and E. E. B. Campbell, *Phys. Rev. Lett.*, 2002, **88**, 097603.
29 O. Albert, S. Roger, Y. Glinec, J. C. Loulergue, J. Etchepare, C. Boulmer-Leborgne, J. Perrière and E. Million, *Appl. Phys. A: Mater. Sci. Process.*, 2003, **76**, 319.
30 J. D. Kmetec, C. L. Gordon III, J. J. Macklin, B. E. Lemoff, G. S. Brown and S. E. Harris, *Phys. Rev. Lett.*, 1992, **68**, 1527.
31 *Handbook of Laser-Induced Breakdown Spectroscopy*, ed. D. A. Cremers and L. J. Radziemski, John Wiley, Hoboken, 2006.

